

Direct observation of a Riedel peak at a YBaCuO end-type Josephson junction

K. Y. Constantinian, L. É. Amatuni, and R. M. Martirosyan

*Institute of Radiophysics and Electronics, Armenian Academy of Sciences,
378410 Ashtarak-2, Armenia*

(Submitted 13 December 1993)

Pis'ma Zh. Eksp. Teor. Fiz. **59**, No. 3, 167–170 (10 February 1994)

The frequency dependence of the amplitude of the oscillatory current $I_1(\Omega)$ of intrinsic Josephson generation at a single YBaCuO end-type junction has been measured by a direct nonresonant method. The current–voltage characteristic of the junction has the shape characteristic of contacts with a direct conductivity. A significantly broadened Riedel peak is observed. An estimate of the attenuation coefficient of the energy gap, $\delta \approx 1.6 \times 10^{-3}$, is insufficiently low.

The transport properties of Josephson junctions formed at grain boundaries in high- T_c superconductors have been the subject of a fair number of studies (e.g., Refs. 1–4). Possible models for the grain boundaries have been discussed in these papers. On the other hand, differences in the conduction mechanism in Josephson junctions of different types can be manifested fairly clearly on a plot of the amplitude (I_1) of the oscillatory Josephson current versus the frequency $\omega = 2\pi f / \omega_g$, where f is the frequency of intrinsic Josephson generation, and $\omega_g = 4\Delta / \hbar$ is a frequency corresponding to the resultant energy of the gap of the Josephson junction.

In this letter we are reporting the results of direct measurements of $i_1 = I_1 / I_c$ as a function of the frequency $\Omega = 2\pi f / \omega_c$, which was varied by varying the temperature. Here ω_c is the characteristic frequency of the Josephson junction, which we used as a “measure” of the value of ω_g in the form $\omega_c = \omega_0 = (2e / \hbar) V_0$, where $V_0 = I_c R_N$, I_c is the critical current, and R_N is the resistance of the Josephson junction in its normal state. These properties were determined from the dc current–voltage characteristic.

The test samples⁵ were prepared by pulsed laser deposition on LaAlO₃(100) substrates with an end-type geometry for the formation of the Josephson junction. The *C*-oriented epitaxial films of YBaCuO, with a thickness of 200 nm, made an angle of 90° at a step 300 nm in height (Ref. 6), which was etched over the entire width of the substrate. The width of the film in the region of the Josephson junction was $\omega \approx 32$ μm . The transition temperatures were $T_c = 79\text{--}83$ K for the Josephson junction and $T_c \geq 86$ K for the electrodes. In the microwave measurements, the substrate, with dimensions of $1.5 \times 0.5 \times 9$ mm, with the Josephson junction formed on it, was placed at the center of a waveguide with a cross section of 11×1 mm. The waveguide was connected to a standard rectangular waveguide with the help of a matching transformer. The spectral power density of the Josephson generation was measured under conditions of broad-band nonresonant matching, with the help of a superheterodyne radiometric receiver, at a frequency $f = 24.7$ GHz. The receiver operated in a two-band regime with a bandwidth $\Delta F = 150$ MHz. At an integration time $\tau = 1$ s, a

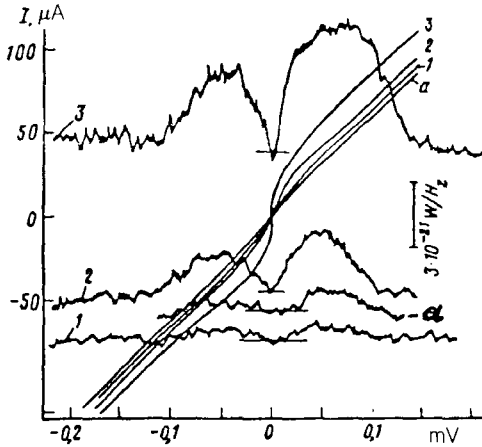


FIG. 1. Current-voltage characteristics and corresponding plots of $S(V)$ for Josephson generation at $f = 24.7$ GHz for an end-type YBaCuO Josephson junction at several temperatures. 1— $T = 78$ K; 2—73.5; 3—69; a—79.1 K (a separate recording). The horizontal straight lines show the zero levels for the $S(V)$ curves. A calibration of $S(V)$ was carried out at a load impedance $R = 2 \Omega$ with $\tau = 1$ s.

sensitivity $\delta S \approx 3 \times 10^{-24}$ W/Hz was achieved. While recording the spectral density of the signal which appeared across the Josephson junction, $S(V)$, we simultaneously measured current-voltage characteristics by the standard four-probe method. We used a battery as a current source and a low-noise analog nanovoltmeter. The leads used to set the current and to measure the potential were attached to the sample by means of gold wire contacts, with subsequent connection to cooled, low-frequency filters and then to "room-temperature" low-frequency filters. The filters were used to eliminate the effect of stray electrical pickup on the characteristics of the Josephson junctions. A multilayer shield made of a permalloy-type alloy was used to shield against the geomagnetic field. The receiver was decoupled from the sample by means of a set of circulators and a waffle-type microwave filter, which suppressed higher harmonics of the beat frequency. The test sample, along with a section of waveguide, was cooled in a closed-loop microcryogenic system. The temperature was monitored within ± 0.1 K near $T \approx 100$ K and considerably more precisely below liquid-nitrogen temperature.

Figure 1 shows some typical current-voltage characteristics and corresponding curves of $S(V)$, recorded over the temperature interval from T_c to $T = 60$ K for a Josephson junction with $T_c = 82$ K, $I_c = 760 \mu\text{A}$, and $R_N = 2.4 \Omega$ at $T = 4.5$ K. The reason for the smearing of these current-voltage characteristics is a thermally activated phase slippage.⁷ For a comparison of the experimental data with the theory, it is desirable that the Josephson junction under study be a single junction and be concentrated at $w \leq 4\lambda_J$, where λ_J is the Josephson penetration depth for a magnetic field.⁸ Although two series-connected grain boundaries should form in the method used here, the first condition holds automatically, since the lower junction is in a superconducting state with $I \ll I_c$ over the entire range of bias currents used experimentally. The second condition holds more rigorously ($w \leq 2\lambda_J$) at $T \geq 69$ K. It can be seen from the figure that the $S(V)$ peaks correspond very accurately to the Josephson relation $V_n = nh/2ef$ for $n = \pm 1$ and $V_1 = 51 \mu\text{V}$. We will not go into the width or shape of the generation line in this letter, but we would like to point out the following. In such a measurement system, we have previously detected⁹ approximately Lorentzian $S(V)$ curves for niobium microbridges. The width of the generation line, Δf , in

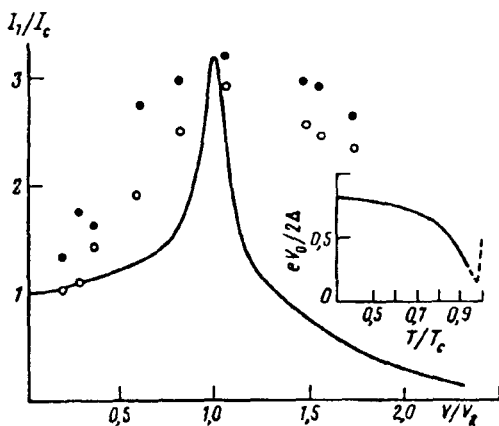


FIG. 2. Experimental values of the normalized Josephson oscillation current I_1/I_c versus the normalized voltage V/V_R , where $V_R = 8V_0$. Filled circles—Results found on the right-hand branch of the current-voltage characteristic; open circles—left-hand branch. The theoretical curve is plotted for a gap attenuation coefficient $\delta = 1.6 \times 10^{-3}$. The inset is a sketch of the temperature dependence $V_0(T)/\Delta(T)$ for a Josephson junction with BCS electrodes.

those previous results was approximately equal to that calculated from the resistive model.⁸ That agreement inspires confidence in the behavior measured here. It is also important to note that the thermally activated phase slippage does not suppress Josephson generation. Furthermore, the measured values of the integrated power, $P = S(V)\Delta f$, with allowance for the mismatch factor $\eta = 4\rho R_d / (\rho + R_d)^2$ (ρ is the characteristic impedance of the microwave line, and R_d is the dynamic resistance of the Josephson junction of the working point), and the loss level in the microwave line, $\alpha \approx 1.1$ dB, correspond to values $i_1 > 1$ at frequencies $\Omega > 1$. We determined values of $I_c(T)$ by a method like that of Ref. 7. Figure shows experimental results on I_1/I_c versus $\Omega = V/V_R$, where V is the voltage across the Josephson junction, and V_R is the voltage corresponding to the maximum of I_1/I_c . We also note that measurements of the peaks of the Shapiro steps for $n=1$ at frequencies $f_e \approx 24, 42$, and 94 GHz at $T=4.5$ K and also at $f_e \approx 56-78$ GHz at $T=35$ K reveal a good agreement between the microwave estimate of the characteristic frequency ω_c and the value of V_0 , which we used for the frequency normalization. Figure also shows a plot of the Riedel peak I_1/I_c versus ω according to theory of Refs. 10 and 11 for tunnel junctions with an attenuation factor $\delta = \Delta'/\Delta = 1.6 \times 10^{-3}$, where Δ and Δ' are respectively the real and imaginary parts of the energy gap. The experimental value $V_R \approx 8V_0$ corresponds to the temperature interval $T/T_c = 0.8-0.9$, where there is also a suppression of ω_c , characteristic of high- T_c superconductors. As the parameter $V_0(T)$ is changed by varying the temperature, a systematic error is introduced because of the different temperature dependences $\Delta(T)$ and $\omega_0(T)$. This systematic error leads to a distortion of the actual shape of the Riedel peak. The inset in Fig. 2 is a qualitative sketch of the temperature-dependent frequency ratio $\omega_0(T)/\omega_g(T)$ for a superconducting tunnel junction with BCS electrodes. The dashed part of the curve is the temperature interval

corresponding to the experiments, in which the ratio ω_0/ω_g is multivalued along the temperature scale. However, this methodological error does not explain the substantial broadening of $i_1(\omega)$. It was shown experimentally in Ref. 12 that polycrystalline YBaCuO has a Gaussian distribution of discrete values Δ_i , spanning the broad voltage range $V \approx 20\text{--}80$ mV. This dynamic range of the voltage, $80/20=4$, is approximately equal to the dynamic range $\Omega_{\max}/\Omega_{\min} \approx 4$, as measured at half the maximum of i_1 . This multivaluedness of the gap can explain both the low value of the experimental estimate of δ , which is typical of tunnel junctions, and the anomalously broad Riedel peak. On the other hand, the current–voltage characteristics of the tunnel junctions studied here, which are clearly not of a tunneling nature, are probably due to the existence of localized wide-gap defects in an insulating layer of a weak-coupling region, which act as centers for a resonant tunneling of unpaired electrons.^{3,13} The noticeable excess current on the current–voltage characteristic over the entire temperature range studied, from 4.5 K to T_c , and the instability of the current–voltage characteristic at low temperatures, $T < 60$ K (at which the condition $w \gg 4\lambda_J$ holds), accompanied by an unstable generation with a significant broadening of the generation line, can be taken as evidence in favor of this mechanism for a shunting of the tunneling characteristic.

We wish to thank A. Braginskii for furnishing the test samples. This study was supported by the Armenian Academy of Sciences and, in part (for K. Y. C. and L. É. A.), by a grant from the Soros International Science Foundation, awarded by the American Physical Society.

¹D. Dimos *et al.*, Phys. Rev. B **41**, 4038 (1990).

²Yu. Xiao-Jun and M. Sayer, Phys. Rev. B **44**, 2348 (1991).

³R. Gross and B. Mayer, Physica C **180**, 235 (1991).

⁴D. K. Lathrop *et al.*, Appl. Phys. Lett. **64**, 228 (1991).

⁵K. Herrman *et al.*, Supercond. Sci. Technol. **4**, 583 (1991).

⁶C. L. Jia *et al.*, Physica C **175**, 545 (1991).

⁷R. Gross *et al.*, Phys. Rev. Lett. **64**, 228 (1990).

⁸K. K. Likharev, *Introduction to the Dynamics of Josephson Junctions* (Nauka, Moscow, 1985).

⁹L. E. Amatuni *et al.*, IEEE Tr. **27**, 2724 (1991).

¹⁰D. J. Scalapino and T. M. Wu, Phys. Rev. Lett. **17**, 315 (1966).

¹¹S. Morita *et al.*, J. Phys. Soc. Jpn. **52**, 617 (1983).

¹²J. E. Núñez-Requeiro and J. M. Aponte, Phys. Rev. B **46**, 1236 (1992).

¹³J. Halbritter, Solid State Commun. **18**, 1447 (1976).

Translated by D. Parsons